

Efficient Conditional Pre-training for Transfer Learning

Shuvam Chakraborty
Department of Computer Science
Stanford University
shuvamc@stanford.edu

Kumar Ayush
Department of Computer Science
Stanford University
kayush@stanford.edu

Evan Sheehan
Department of Computer Science
Stanford University
esheehan@stanford.edu

Burak Uzkent
Department of Computer Science
Stanford University
buzkent@cs.stanford.edu

Kumar Tanmay
Department of Computer Science
IIT Kharagpur
kr.tanmay147@iitkgp.ac.in

Stefano Ermon
Department of Computer Science
Stanford University
ermon@cs.stanford.edu

Abstract

Almost all the state-of-the-art neural networks for computer vision tasks are trained by (1) pre-training on a large-scale dataset and (2) finetuning on the target dataset. This strategy helps reduce dependence on the target dataset and improves convergence rate and generalization on the target task. Although pre-training on large-scale datasets is very useful, its foremost disadvantage is high training cost. To address this, we propose efficient filtering methods to select relevant subsets from the pre-training dataset. Additionally, we discover that lowering image resolutions in the pre-training step offers a great trade-off between cost and performance. We validate our techniques by pre-training on ImageNet in both the unsupervised and supervised settings and finetuning on a diverse collection of target datasets and tasks. Our proposed methods drastically reduce pre-training cost and provide strong performance boosts. Finally, we improve standard ImageNet pre-training by 1-3% by tuning available models on our subsets and pre-training on a dataset filtered from a larger scale dataset.

1. Introduction

Many modern computer vision methods rely heavily on large-scale labeled datasets, which are often costly and time-consuming to collect [23, 14, 4]. Alternatives to reducing dependency on large-scale labelled data include pre-training a network on the publicly available ImageNet

dataset with labels [8]. It has been shown that ImageNet features can transfer well to many different target tasks [18, 39, 29, 16, 19]. Another alternative, unsupervised learning, has received tremendous attention recently with the availability of extremely large-scale data with no labels, as such data is costly to obtain [23]. It has been shown that recent unsupervised learning methods, e.g. contrastive learning, can perform on par with their supervised learning counterparts [14, 15, 12, 2, 3, 4]. Additionally, it has been shown that unsupervised learning methods perform better than pre-training on ImageNet on various downstream tasks [14, 28, 15, 4]

The explosion of data quantity and improvement of unsupervised learning portends that the standard approach in future tasks will be to (1) learn weights on a very large-scale dataset with unsupervised learning and (2) fine-tune the weights on a small-scale target dataset. A major problem with this approach is the large amount of computational resources required to train a network on a very large scale dataset [23]. For example, a recent contrastive learning method, MoCo-v2 [15, 14], uses 8 Nvidia-V100 GPUs to train on ImageNet-1k for 53 hours, which can cost thousands of dollars. Extrapolating, this forebodes pre-training costs on the order of millions of dollars when considering much larger-scale datasets. Those without access to such resources will require selecting relevant subsets of those datasets. However, other studies that perform conditional filtering, such as [40, 7, 24, 11], do not take efficiency into account.

Cognizant of these pressing issues, we propose novel

methods to efficiently *filter* a user defined number of pre-training images conditioned on a target dataset as well as a novel sequential pre-training method for our methods to work efficiently in practical settings with several target tasks. We also investigate the use of low resolution images for pre-training, which we find provides a great cost to performance trade-off. Our approach consistently outperforms other methods by 2-9% and are both flexible, translating to both supervised and unsupervised settings, and adaptable, translating to a wide range of target tasks including image recognition, object detection and semantic segmentation. Due to our focus on filtering based on image features, not labels, our methods perform especially well in the more relevant unsupervised setting, where pre-training on a 12% subset of data can achieve within 1-4% of full pre-training target task performance. Additionally, we use our methods to tune ImageNet pre-trained models and filter from larger scale data to improve on standard ImageNet pre-training by 1-3% on downstream tasks. Given these results and the exponentially growing scale of unlabeled data, our methods can replace the standard ImageNet pre-training with a target task specific efficient conditional pre-training.

2. Related Work

Active Learning The goal in active learning is to fit a function by selectively querying labels for samples where the function is currently uncertain. In a basic setup, the samples with the highest entropies are chosen for annotation [37, 10, 1, 27]. The model is iteratively updated with these samples and accordingly selects new samples. Active learning typically assumes similar data distributions for candidate samples, whereas our data distributions can potentially have large shifts. Furthermore, active learning, due to its iterative nature, can be quite costly, hard to tune, and can require prior distributions [25].

Unconditional Transfer Learning The success of deep learning on datasets with increased sample complexity has brought transfer learning to the attention of the research community. Pre-training networks on ImageNet-1k has been shown to be a very effective way of initializing weights for a target task with small sample size [18, 39, 29, 16, 19, 34, 32]. However, all these studies use unconditional pre-training as they employ the weights pre-trained on the full ImageNet dataset for any target task, and, as mentioned, full pre-training on large scale data could be prohibitively costly.

Conditional Transfer Learning [40, 7, 24], on the other hand, filter the pre-training dataset conditioned on target tasks. In particular, [7, 11] use greedy class-specific clustering based on feature representations of target dataset images. To learn image representations, they use an encoder trained on the massive JFT-300M dataset [17]. It should be highlighted that pre-training on JFT-300M dataset to learn

encoder for filtering source images dramatically increases complexity. [40] trains a number of expert models on many subsets of the pre-training dataset. Source images are assigned high importance weights if they are used for the training of an expert with a good target task performance. However, this method is computationally expensive as it requires training many experts on different subsets of the pre-training dataset and fine-tuning them on the target dataset to assign importance weights to source images.

Our methods differ from the past works as we take into account both pre-training dataset filtering efficiency and target task performance.

3. Problem Definition and Setup

We assume a target task dataset represented as $\mathcal{D}_t = (\mathcal{X}_t, \mathcal{Y}_t)$ where $\mathcal{X}_t = \{x_t^1, x_t^2, \dots, x_t^M\}$ represents a set of M images with their ground truth labels \mathcal{Y}_t . Our goal is to train a function f_t parameterized by θ_t on the dataset \mathcal{D}_t to learn $f_t : x_t^i \mapsto y_t^i$. One strategy is using randomly initialized weights for θ_t , but a better recipe exists for a small size dataset \mathcal{D}_t . In this case, we first pre-train θ_t on a large-scale source dataset \mathcal{D}_s and fine-tune θ_t on \mathcal{D}_t . This strategy not only reduces the amount of labeled samples needed in \mathcal{D}_t but also boosts the accuracy in comparison to the randomly initialized weights [23, 33]. For the pre-training dataset, we can have either labelled or unlabelled setups: (1) $\mathcal{D}_s = (\mathcal{X}_s, \mathcal{Y}_s)$ and (2) $\mathcal{D}_s = (\mathcal{X}_s)$ where $\mathcal{X}_s = \{x_s^1, x_s^2, \dots, x_s^N\}$. The most common example of the labelled setup is the ImageNet dataset [8]. However, it is tough to label vast amounts of publicly available images, and with the increasing popularity of unsupervised learning methods [4, 5, 3, 14, 15], it is easy to see that unsupervised pre-training on very large \mathcal{D}_s with no ground-truth labels will be the standard and preferred practice in the future.

A major problem with learning θ_t on a very large-scale dataset \mathcal{D}_s is the computational cost, and using the whole dataset may be impossible for most. One way to reduce costs is to filter out images deemed less relevant for \mathcal{D}_t to create a dataset $\mathcal{D}'_s \in \mathcal{D}_s$ where $\mathcal{X}_s = \{x_s^1, x_s^2, \dots, x_s^{N'}\}$ represents a filtered version of \mathcal{D}_s with $N' \ll N$. Our approach conditions the filtering step on the target dataset \mathcal{D}_t . In this study, we propose flexible and adaptable methods to perform *efficient conditional pre-training*, which reduces the computational costs of pre-training and maintains high performance on the target task.

4. Methods

We investigate a variety of methods to perform efficient pre-training while maintaining high performance on the target dataset. We visualize our overall procedure in Figure 1 and explain our techniques below.

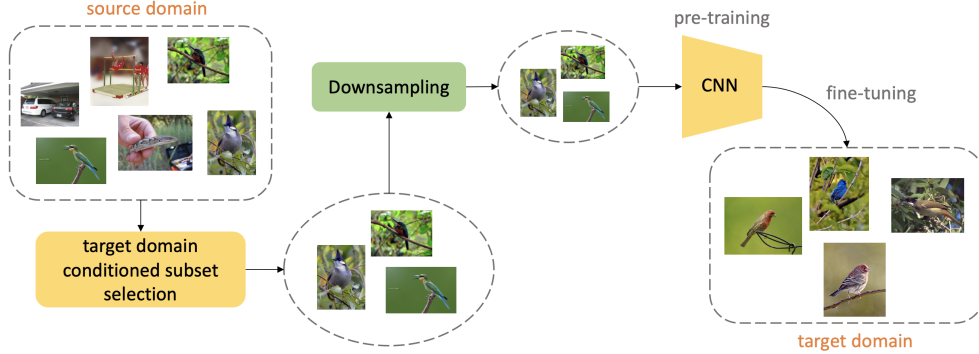


Figure 1: Schematic overview of our approach. We first perform a conditional filtering method on the source dataset and downsample image resolution on this filtered subset. Finally, we perform pre-training on the subset and finetuning on the target task.

4.1. Conditional Data Filtering

We propose novel methods to perform conditional filtering efficiently. Our methods score every image in the source domain and select the best scoring images according to a pre-specified data budget N' . Our methods are fast, requiring at most one forward pass through \mathcal{D}_s to get the filtered dataset \mathcal{D}'_s and can work on both $\mathcal{D}_s = (\mathcal{X}_s, \mathcal{Y}_s)$ and $\mathcal{D}_s = (\mathcal{X}_s)$. The fact that we consider *data features not labels* perfectly lends our methods to the more relevant unsupervised setting. This is in contrast to previous work such as [7, 11, 24] which do not consider efficiency and are designed primarily for the supervised setting and thus will be more difficult for most to apply to large scale datasets.

Algorithm 1 Clustering Based Filtering

- 1: **procedure** CLUSTERFILTER($\mathcal{D}_s, \mathcal{D}_t, N', K, \text{AggOp}$)
 - 2: $f_h \leftarrow \text{TRAIN}(\mathcal{D}_t)$ \triangleright Train Feature Extractor
 - 3: $\mathcal{Z}_t \leftarrow \{f_h(x_t^i)\}_{i=1}^M$ \triangleright Target Representations
 - 4: $\{\hat{z}\}_{k=1}^K \leftarrow K\text{-Means}(\mathcal{Z}_t, K)$ \triangleright Cluster Target
 - 5: $d_k^i \leftarrow \|f_h(x_s^i) - \hat{z}_k\|_2$ \triangleright Source Distances
 - 6: $c_s \leftarrow \{\text{AggOp}(\{d_k^i\}_{k=1}^K)\}_{i=1}^N$ \triangleright Score Source
 - 7: $\mathcal{D}'_s \leftarrow \text{BOTTOM}(\mathcal{D}_s, N', c_s)$ \triangleright Filter Source
 - 8: **return** \mathcal{D}'_s \triangleright Return the Filtered Subset
-

4.1.1 Conditional Filtering by Clustering

Selecting an appropriate subset \mathcal{D}'_s of pre-training data \mathcal{D}_s can be viewed as selecting a set of data that minimizes some distance metric between \mathcal{D}'_s and the target dataset \mathcal{D}_t , as explored in [7, 11]. This is accomplished by taking feature representations \mathcal{Z}_s of the set of images \mathcal{X}_s and selecting pre-training image classes which are close (by some distance metric) to the representations of the target dataset classes. Building on this, we make several significant modifications

to account for our goals of efficiency and application to unsupervised settings.

Training Only with Target Data. We do not train a network f_h on a large scale dataset, i.e. JFT-300M [7], as this defeats the entire goal of pre-training efficiency. Therefore, we first train a model f_h with parameters θ_h using the target dataset $\mathcal{D}_t = (\mathcal{X}_t, \mathcal{Y}_t)$ and use the learned θ_h to filter the source dataset \mathcal{D}_s .

Consider Source Images Individually. Selecting entire classes of pre-training data can be suboptimal when limited to selecting a small subset of the data. For example, if limited to 6% of ImageNet, (a reasonable budget for massive datasets), we can only select 75 of the 1000 classes, which may prohibit the model from having the breadth of data needed to learn transferrable features. Instead, we treat each image x_s^i from \mathcal{D}_s separately to flexibly over-represent relevant classes while not being forced to select entire classes. Additionally, very large scale datasets may not have class labels \mathcal{Y}_s . For this reason, we want to develop methods that work with unsupervised learning, and treating source images independently accomplishes this.

Scoring and Filtering. Finally, we choose to perform K-Means clustering on the representations \mathcal{Z}_t learned by f_h to get K cluster centers $\{\hat{z}\}_{k=1}^K$. We then compute the distances between \mathcal{X}_s and $\{\hat{z}\}_{k=1}^K$ as

$$d_k^i(x_s^i, k) = \|f_h(x_s^i; \theta_h) - \hat{z}_k\|_p \quad (1)$$

where p is typically 1 or 2 (L1 or L2 distance). We can score x_s^i by considering an *Aggregation Operator*(AggOp) of either average distance to the cluster centers

$$c_s^i = \frac{1}{K} \sum_{k=1}^K d_k^i \quad (2)$$

or minimum distance

$$c_s^i = \min(\{d_k^i\}_{k=1}^K). \quad (3)$$

To filter, we sort by c'_s in ascending order and select N' images to create $\mathcal{D}'_s \in \mathcal{D}_s$ and pre-train θ_t on it.

Advantages of our Method Performing unsupervised clustering ensures that our method is not fundamentally limited to image recognition target tasks and also does not assume that source dataset images in the same class should be grouped together. Furthermore, our method requires only a relatively cheap single forward pass through the pre-training dataset. It attains our goals of efficiency and flexibility, in contrast to prior work such as [11, 7]. We outline the algorithm step-by-step in Algorithm 1 and lay out the method visually in the Appendix.

Algorithm 2 Domain Classifier Filtering

```

1: procedure DOMAINCLSFILTER( $\mathcal{D}_s, \mathcal{D}_t, N'$ )
2:   SAMPLE  $\{x_s^i\}_{i=1}^M \in \mathcal{D}_s$ 
3:    $\mathcal{X}_h \leftarrow \{\{x_s^i\}_{i=1}^M, \{x_t^i\}_{i=1}^M\}$ 
4:    $\mathcal{Y}_h \leftarrow \{\{0\}_{i=1}^M, \{1\}_{i=1}^M\}$   $\triangleright$  Domain Labels
5:    $\mathcal{D}_h \leftarrow (\mathcal{X}_h, \mathcal{Y}_h)$   $\triangleright$  Training Data
6:    $f_h(x; \theta_h) \leftarrow \operatorname{argmin}_{\theta_h} CELoss(\mathcal{D}_h)$   $\triangleright$  Fit Model
7:    $c_s \leftarrow \{f_h(x_s^i; \theta_h)\}_{i=1}^M$   $\triangleright$  Score
8:    $\mathcal{D}'_s \leftarrow TOP(\mathcal{D}_s, N', c_s)$   $\triangleright$  Filter Source
9:   return  $\mathcal{D}'_s$   $\triangleright$  Return the Filtered Subset

```

4.1.2 Conditional Filtering with Domain Classifier

In this section, we propose a novel domain classifier to filter \mathcal{D}_s with several desirable attributes. We outline the algorithm step-by-step in Algorithm 2 and provide a depiction in the Appendix.

Training. In this method, we propose to learn θ_h to ascertain whether an image belongs to \mathcal{D}_s or \mathcal{D}_t . θ_h is learned on a third dataset $\mathcal{D}_h = (\mathcal{X}_h, \mathcal{Y}_h)$ where $\mathcal{X}_h = \{\{x_s^i\}_{i=1}^M, \{x_t^i\}_{i=1}^M\}$, $M = |\mathcal{D}_t|$, consisting of full set of \mathcal{D}_t and a small random subset of \mathcal{D}_s . Each source image $x_s^i \in \mathcal{X}_s$ receives a negative label and each target image $x_t^i \in \mathcal{X}_t$ receives a positive label giving us the label set $\mathcal{Y}_h = \{\{0\}_{i=1}^M, \{1\}_{i=1}^M\}$. We then learn θ_h on \mathcal{D}_h using cross entropy loss as

$$\operatorname{argmin}_{\theta_h} \sum_{i=1}^{2M} y_h^i \log(f_h(x_h^i; \theta_h)) + (1 - y_h^i) \log(1 - f_h(x_h^i; \theta_h)). \quad (4)$$

Scoring and Filtering. Once we learn θ_h we obtain the confidence score $p(y_h = 1|x_s^i; \theta_h)$ for each image $x_s^i \in \mathcal{X}_s$. We then sort the source images \mathcal{X}_s in descending order based on $p(y_h = 1|x_s^i; \theta_h)$ and choose the top N' images to create the subset $\mathcal{D}'_s \in \mathcal{D}_s$.

Interpretation. Our method can be interpreted as selecting images from the pre-training domain with high probability of belonging to the target domain. It can be shown

[13] that the Bayes Optimal binary classifier \hat{f}_h assigns probability

$$p(y_h = 1|x_s^i; \theta_h) = \frac{p_t(x_s^i)}{p_s(x_s^i) + p_t(x_s^i)} \quad (5)$$

for an image $x_s^i \in \mathcal{X}_s$ to belong to the target domain, where p_t and p_s are the true data probability distributions for the target and source domains respectively.

Algorithm 3 Sequential Pre-training

```

1: procedure SEQUENTIALPRE-TRAIN( $\mathcal{T}, \mathcal{T}_{sem}, \mathcal{S}, N'$ )
2:    $f = \text{RAND}()$   $\triangleright$  Randomly Initialize Model
3:   while  $True$  do  $\triangleright$  Handle All Tasks
4:      $\mathcal{T}_{sem}.wait()$   $\triangleright$  Wait for Task Semaphore
5:      $\mathcal{S}, D_i = \mathcal{T}.pop()$   $\triangleright$  Current Task from Queue
6:      $\mathcal{S}'_i = \text{FILTER}(\mathcal{D}_i, \mathcal{S}, N')$ 
7:      $f = \text{TRAIN}(f, \mathcal{S}'_i)$   $\triangleright$  Update Model
8:      $\text{TASK}(f, \mathcal{D}_i, T_i)$   $\triangleright$  Perform Current Task

```

4.2. Sequential Pre-training

The methods we present work efficiently for a single target task. However, in practice, we may be interested in many different target tasks, and performing separate pre-training from scratch for each one may be prohibitively inefficient. As a result, we propose performing sequential pre-training, where we leverage previously trained models to more quickly learn better transfer learning representations.

Formally, we assume that we have a large scale source dataset S (which can potentially grow over time) and want to perform tasks on N target datasets, which we receive sequentially over time as $((S, D_1, t_1), (S, D_2, t_2), \dots, (S, D_N, t_N))$. We receive our first task with dataset D_1 at time t_1 , and we conditionally filter S into S'_1 based on our data budget. Then, we pre-train a model, f_1 , from scratch on S'_1 , and perform task one. Generally, when we receive D_i at time t_i , we filter S conditioned on D_i to obtain S'_i . Then, we take our last pre-trained model f_{i-1} and update its weights on S'_i to obtain f_i , which we separately use to perform the task on D_i . Subsequent tasks require smaller and smaller amounts of additional pre-training, thus drastically reducing the total epochs required for multiple tasks and making our methods feasible in practical settings. We lay out this procedure step by step in Algorithm 3.

4.3. Adjusting Pre-training Spatial Resolution

To augment our methods, we propose changing spatial resolution of images \mathcal{X}_s in the source dataset \mathcal{D}_s while pre-training. We assume that an image is represented as $x_s^i \in \mathbb{R}^{W_s \times H_s}$ or $x_t^i \in \mathbb{R}^{W_t \times H_t}$ where W_s, W_t , where H_s

and H_t represent image width and height. Traditionally, after augmentations, we use $W_s, W_t = 224$ and $H_s, H_t = 224$. Here, we consider decreasing W_s and H_s on the pre-training task while maintaining $W_t, H_t = 224$ on the target task. Reducing image resolution while pre-training can provide significant speedups by decreasing FLOPs required by convolution operations, and our experiments show that downsizing image resolution by half $W_s, H_s = 112$ almost halves the pre-training time.

Training on downsized images and testing on higher resolution images due to geometric camera effects on standard augmentations has previously been explored [30]. Our setting is not as amenable to the same analysis, as we have separate data distributions \mathcal{D}_s and \mathcal{D}_t captured under different settings. Nevertheless, we show low resolution training is still an effective method in the transfer learning setting.

5. Experiments

In our experiments, we report finetuning performance for combinations of resolution, pre-training budget, and filtering method as well as performance with full pre-training and no pre-training for reference.

5.1. Datasets

5.1.1 Source Dataset

For our primary source dataset, we utilize ImageNet-2012 [8], with $\sim 1.28\text{M}$ images over 1000 classes. We experiment under two data budgets, limiting filtered subsets to 75K ($\sim 6\%$) and 150K ($\sim 12\%$) ImageNet images. This is an appropriate proportion when dealing with pre-training datasets on the scale of tens of millions or more images.

5.1.2 Target Datasets

Image Recognition As target datasets, we utilize the Stanford Cars [38] dataset, the Caltech Birds [20] dataset, and a subset of the Functional Map of the World [6] (fMoW) dataset. We provide basic details about these datasets in the **Appendix**. These datasets have different degrees of variation and images per class and lend important diversity to validate the flexibility of our methods. Cars has a fairly small distribution shift from ImageNet, and pre-training on ImageNet performs well on it, but Birds contains a larger shift and datasets emphasizing natural settings such as iNat perform better [7, 36]. Finally, fMoW, consisting of overhead satellite images, contains images very dissimilar to ImageNet. Additionally, Birds and Cars are fine grained, discriminating between different species of birds or models of cars, respectively. In contrast, fMoW is much more general, describing buildings or landmarks [26, 35, 31].

Detection and Segmentation [14, 15] show that unsupervised ImageNet pre-training is most effective when

paired with more challenging low level downstream tasks. Therefore, we also perform experiments in the object detection and semantic segmentation setting to validate the flexibility and adaptability of our methods. To this end, we utilize the Pascal VOC [9] dataset with unsupervised ImageNet pre-training of the backbone.

5.2. Analyzing Filtering Methods

Here, we make some important points about our filtering methods and refer the reader to the **Appendix** for specific implementation details.

Domain Classifier Accuracy We typically train the domain classifier to 92-95% accuracy. We empirically find this is the "sweet spot" as classifiers with 88-90% accuracy, perhaps due to not learning relevant features, and 98+% accuracy, perhaps due to over-discriminating minor differences between domains such as noise or color/contrast, do not perform as well.

Efficiency and Adaptability Comparison. The domain classifier trains a simple binary classifier and bypasses full representation learning on a target dataset, computing distances, or clustering. However, this difference in efficiency is small compared to pre-training cost. More importantly, when the target task is not image level classification, the representation learning step for clustering based filtering must be modified in a non-trivial manner. This can involve a global pool over spatial feature maps while performing object detection or an entirely different setup like unsupervised learning. The domain classifier is more adaptable than clustering as it does not require modification for any type of target task.

Qualitative Analysis. In Figures 2 and 3, we visualize some of the highest scoring filtered images for all our methods on classification tasks and verify that our filtering methods do select images with *relevant features* to the target task. Unsurprisingly, more interpretable images are selected for Birds and Cars, as there are no satellite images in ImageNet. Nevertheless, we see that the selected images for fMoW still contain *relevant features* such as color, texture, and shapes.

5.3. Transfer Learning for Image Recognition

We first apply our methods to the task of image classification with both supervised and unsupervised pre-training. We detail our results below.

5.3.1 Supervised Pre-training Results

We present target task accuracy for all our methods on Cars, Birds, and fMoW along with approximate pre-training and filtering time in Table 1.

Effect of Image Resolution. We see that downsizing pre-training resolution produces gains of up to .5% in clas-

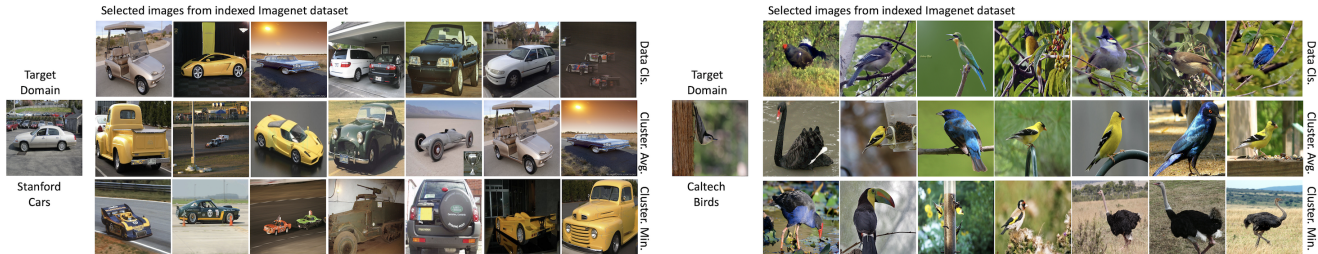


Figure 2: High scoring ImageNet samples selected by all our conditional filtering methods for target datasets Stanford Cars and Caltech Birds.

Supervised Pre-train.		Target Dataset			Cost (hrs)
224 x 224		Small Shift	Large Shift		
Pre-train. Sel. Method		Cars	Birds	fMow	
0%	Random Init.	52.89	42.17	43.35	0
100%	Entire Dataset	82.63	74.87	59.05	160-180
6%	Random	72.2	57.87	50.25	30-35
	Domain Cls.	74.37	59.73	51.17	35-40
	Clustering (Avg)	73.64	56.33	51.14	40-45
	Clustering (Min)	74.23	57.67	50.27	40-45
12%	Random	76.12	62.73	53.28	45-50
	Domain Cls.	76.18	64	53.41	50-55
	Clustering (Avg)	77.12	61.73	53.12	55-60
	Clustering (Min)	75.81	64.07	52.91	55-60

Supervised Pre-train.		Target Dataset			Cost (hrs)
112 x 112		Small Shift	Large Shift		
Pre-train. Sel. Method		Cars	Birds	fMow	
0%	Random Init.	52.89	42.17	43.35	0
100%	Entire Dataset	83.78	73.47	57.39	90-110
6%	Random	72.76	57.4	49.73	15-20
	Domain Cls.	73.66	58.73	50.66	20-25
	Clustering (Avg)	74.53	56.97	51.32	25-30
	Clustering (Min)	71.72	58.73	49.06	25-30
12%	Random	75.4	62.63	52.59	30-35
	Domain Cls.	76.36	63.5	53.37	35-40
	Clustering (Avg)	77.53	61.23	52.67	40-45
	Clustering (Min)	76.36	63.13	51.6	40-45

Table 1: Target task accuracy and approximate filtering and pre-training cost(time in hrs on 1 GPU) on 3 visual categorization datasets obtained by pre-training on different subsets of the source dataset (ImageNet) with different filtering methods at different resolutions.

MoCo-v2 [15]		Target Dataset			Cost (hrs)
224 x 224		Small Shift	Large Shift		
Pre-train. Sel. Method		Cars	Birds	fMow	
0%	Random Init.	52.89	42.17	43.35	0
100%	Entire Dataset	83.52	67.49	56.11	210-220
6%	Random	75.70	56.82	52.53	20-25
	Domain Cls.	78.67	61.55	52.96	23-28
	Clustering (Avg)	78.66	60.88	53.19	25-30
	Clustering (Min)	79.45	59.36	53.5	25-30
12%	Random	75.66	61.70	53.56	30-35
	Domain Cls.	78.68	63.08	54.01	33-38
	Clustering (Avg)	78.68	62.53	54.4	35-40
	Clustering (Min)	79.55	63.6	54.26	35-40

MoCo-v2 [15]		Target Dataset			Cost (hrs)
112 x 112		Small Shift	Large Shift		
Pre-train. Sel. Method		Cars	Birds	fMow	
0%	Random Init.	52.89	42.17	43.35	0
100%	Entire Dataset	84.09	66.57	56.83	110-120
6%	Random	75.38	56.63	52.59	10-15
	Domain Cls.	76.84	57.93	53.3	13-18
	Clustering (Avg)	76.86	58.4	53.75	15-20
	Clustering (Min)	77.53	57.1	53.83	15-20
12%	Random	78.35	61.50	54.28	15-20
	Domain Cls.	80.38	63.93	54.53	18-23
	Clustering (Avg)	80.21	63.50	55.06	20-25
	Clustering (Min)	79.63	62.77	55.03	20-25

Table 2: Target task accuracy and approximate filtering and pre-training cost(time in hrs on 4 GPUs) on 3 visual categorization datasets obtained by pre-training on different subsets of the source dataset (ImageNet) with different filtering methods at different resolutions.

sification accuracy on Cars and less than 1% drop in accuracy on Birds and fMoW, while being 30-50% faster than full pre-training. These trends suggest that training on lower resolution images can help the model learn more generalizable features for similar source and target distributions. This effect erodes slightly as we move out of distribution,

however pre-training on lower resolution images offers an attractive trade-off between efficiency and accuracy in all settings.

Impact of Filtering. We find that our filtering techniques consistently provide up to a 2.5% performance increase over random selection, with a relatively small in-

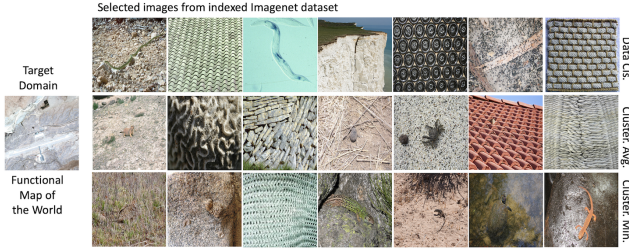


Figure 3: High scoring ImageNet samples selected by all our conditional filtering methods for fMoW.

crease in cost. Unsurprisingly, filtering provides the most gains on Cars and Birds where the target dataset has a smaller shift. On fMoW, it is very hard to detect *similar* images to ImageNet, as the two distributions have very little overlap. Nevertheless, in this setting, our filtering methods can still select enough relevant features to provide a 1-2% boost.

Comparison of Filtering Methods. While all our methods perform well, applying a finer lens, we see that the domain classifier is less variable than clustering and always outperforms random selection. On the other hand, average clustering performs well on Cars or fMoW, but does worse than random on Birds and vice versa for min clustering. These methods rely on computing high dimensional vector distances to assign a measure of similarity, which may explain their volatility since such high dimensional distances are not considered in supervised pre-training.

5.3.2 Unsupervised Pre-training Results

We observe promising results in the supervised setting, but as explained, a more realistic and useful setting is the unsupervised setting due to the difficulties inherent in collecting labels for large-scale data. Thus, we use MoCo-v2 [15], a state-of-the-art unsupervised learning method, to pre-train on ImageNet and present results for Cars, Birds, and fMoW in Table 2.

Effect of Image Resolution. We find that in the unsupervised setting, with 150K pre-training images, lower resolution pre-training largely maintains or even improves performance as the target distribution shifts. Unsupervised pre-training relies more on high level features and thus may be better suited than supervised methods for lower resolution pre-training, since higher resolution images may be needed to infer fine grained label boundaries.

Increased Consistency of Clustering. Relative to the supervised setting, clustering based filtering provides more consistent performance boosts across the different settings and datasets. It is possible that clustering based filtering may be well suited for unsupervised contrastive learning techniques, which also rely on high dimensional feature dis-

tances.

Impact of Filtering. Our filtering techniques aim to separate the image distributions based on the true image distributions and feature similarity, not label distribution (which may not be observable). Unsupervised learning naturally takes advantage of our filtering methods, and we see gains of up to 5% over random filtering in the 75K setting and up to 4% in the 150K setting, a larger boost than during supervised pre-training. This leads to performance that is within 1-4% of full unsupervised pre-training but close to 10 times faster, due to using a 12% subset. These results are notable, because, as mentioned, we anticipate that unsupervised learning will be the default method for large-scale pre-training and our methods can approach full pre-training while significantly reducing cost.

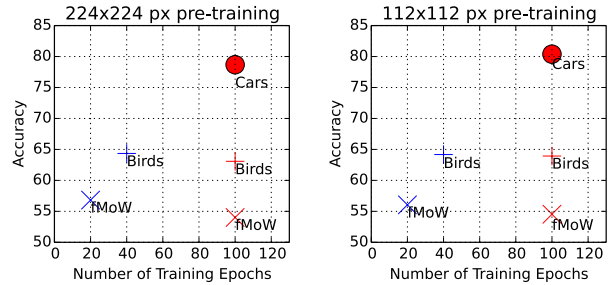


Figure 4: Results for sequential pre-training (blue) vs independent pre-training (red). Our sequential method requires fewer epochs over time and performs better than independent pre-training.

5.3.3 Sequential Pre-training

Cognizant of the inefficiencies of performing independent pre-training with many target tasks, we assume a practical scenario where we receive three tasks, D_1, D_2, D_3 representing Cars/Birds/fMoW respectively, with S being ImageNet. We use the domain classifier to filter 150K images, obtain S'_1, S'_2, S'_3 , and sequentially pre-train for 100, 40, and 20 epochs respectively with MoCo-v2.

We present results in Figure 4. Naturally, for Cars the results do not change, but since learned features are leveraged, not discarded, for subsequent tasks, we observe gains of up to 1% on Birds and 2% on fMoW over Table 2 while using 160 total pre-training epochs vs 300 for independent pre-training. Our sequential pre-training method augments the effectiveness of our filtering methods in settings with many target tasks over time and drastically reduces the number of epochs required. We leave the application of this technique for object detection and segmentation as future work.

Detection		224x224			112x112		
Pre-train. Sel. Method		AP	AP50	AP75	AP	AP50	AP75
0%	Random Init.	14.51	31.00	11.62	14.51	31.00	11.62
100%	Entire Dataset	43.94	73.05	45.96	43.62	72.56	45.52
6%	Random	29.01	54.02	27.26	28.10	52.82	26.39
	Domain Cls.	30.47	56.58	29.04	31.19	56.90	30.43
	Clustering (Avg)	30.61	55.65	28.75	30.13	55.01	29.47
	Clustering (Min)	30.44	56.11	29.46	30.39	55.89	28.18
12%	Random	30.84	52.07	29.15	30.56	56.1	29.04
	Domain Cls.	34.41	61.85	33.36	34.98	61.83	35.02
	Clustering (Avg)	32.34	56.24	31.28	32.01	57.16	33.48
	Clustering (Min)	32.58	57.77	31.16	32.96	58.25	33.64

Segmentation		224x224			112x112		
Pre-train. Sel. Method		mIOU	mAcc	allAcc	mIOU	mAcc	allAcc
0%	Random Init.	0.45	0.55	0.82	0.45	0.55	0.82
100%	Entire Dataset	0.65	0.74	0.89	0.63	0.72	0.88
6%	Random	0.55	0.65	0.85	0.58	0.68	0.87
	Domain Cls.	0.62	0.70	0.88	0.62	0.70	0.88
	Clustering (Avg)	0.61	0.70	0.88	0.59	0.69	0.87
	Clustering (Min)	0.61	0.70	0.88	0.61	0.70	0.88
12%	Random	0.56	0.65	0.86	0.59	0.69	0.87
	Domain Cls.	0.65	0.74	0.89	0.62	0.71	0.89
	Clustering (Avg)	0.64	0.73	0.89	0.59	0.68	0.87
	Clustering (Min)	0.61	0.70	0.88	0.61	0.70	0.88

Table 3: Comparison of different filtering methods and resolutions on transfer learning on Pascal-VOC detection and segmentation. For object detection and semantic segmentation, we use unsupervised pre-training method MoCo-v2 [15].

5.4. Transfer Learning for Low Level Tasks

Previously we explored image level classification target tasks for conditional pre-training. In this section, we perform experiments on transfer learning for object detection and semantic segmentation on the Pascal VOC dataset.

We present results in Table 3. For filtering, we use the domain classifier with no modifications and for clustering, we use MoCo-v2 on Pascal VOC to learn representations. We refer the reader to the **Appendix** for more experimental details.

Effect of Image Resolution. Overall, we see pre-training on low resolution images produces no overall decrease in performance, with the usual corresponding 30-50% reduction in training time, confirming the adaptability of pre-training on lower resolution images for more challenging lower level tasks.

Adaptability Comparison Relative to prior work [7, 40], our clustering method is more adaptable and can efficiently be used for detection/segmentation as well as image classification. However, the representation learning step for clustering must be changed for such target tasks, which can hinder downstream performance as a representation learning technique like MoCo-v2 may be more challenging on smaller scale datasets like Pascal VOC. The domain classifier, on the other hand, avoids these challenges and does not have to change when the target task is changed.

Performance Comparison We observe that all of our proposed filtering techniques yield consistent gains of up to 9% over random filtering, confirming their applicability to lower level tasks. In the segmentation setting, pre-training on a 12% subset can match full pre-training performance. Clustering produces meaningful gains, but the domain classifier outperforms it in almost every object detection scenario and the majority of segmentation metrics. This is especially pronounced with a larger pre-training subset, showing the domain classifier can effectively filter more relevant images.

ImageNet+		224x224			112x112		
Pre-train. Sel. Method		Cars	Birds	fMow	Cars	Birds	fMow
ImageNet		83.52	67.49	56.11	84.09	66.57	56.83
ImageNet+Domain Cls.		84.33	69.78	57.95	84.56	69.88	58.04

Table 4: Classification results for ImageNet+. By fine-tuning ImageNet weights on our ImageNet filtered subset, we can improve ImageNet pre-training performance on downstream classification tasks.

5.5. Improving on Full ImageNet Pre-training

Thus far, we have used ImageNet as a proxy for a very large scale dataset where full pre-training would be infeasible, and we show the promise of our methods in pre-training on subsets of ImageNet. We note that pre-trained models on ImageNet (1.28M images) are readily available, so we motivate practical use of our method by showing how they can outperform full ImageNet pre-training.

ImageNet+ Here, we take a model pre-trained on ImageNet and help it focus on specific examples with relevant features by tuning its weights for a small additional number of epochs on our conditionally filtered subsets before transfer learning. We find this is effective in the unsupervised setting due to its focus on image features without label distributions, as mentioned previously. Thus, we apply this method to Cars/Birds/fMoW and tune pre-trained ImageNet weights with MoCo-v2 for 20 additional epochs on 150K domain classifier filtered ImageNet subsets. We present results in Table 4 and report improvements by up to 1-3% over full ImageNet pre-training, a strong performance increase for minimal extra cost.

Large Scale Filtering Here, we improve on full ImageNet by filtering a similar number of images from a larger scale dataset. To this end, we assemble a large scale dataset consisting of 6.71M images from the Places, OpenImages, ImageNet, and MSCOCO datasets [22, 41, 21] and filter 1.28M images using the domain classifier conditioned on the Cars dataset. We pre-train using MoCo-v2 and present

	Random@224	LargeScale@112	LargeScale@224	ImageNet@224
Accuracy	82.96	84.29	84.51	83.52
Cost (hrs)	210-220	130-140	230-240	210-220

Table 5: Results on large scale experiments. Filtering a large scale dataset with the domain classifier improves accuracy on the Stanford Cars dataset over a random subset and ImageNet with about 10% more cost at 224 pixels resolution. and 35% savings at 112 pixels resolution.

our accuracy on the Cars dataset in Table 5. Our filtering methods improve on the current default of 224 resolution ImageNet pre-training by 1-1.5% with good cost tradeoffs. Interestingly, a random subset of the large scale dataset performs worse than ImageNet, showing that our filtering method is crucial to select relevant examples. We also note that previously, for classification, our filtering methods saw larger gains with 6% than 12% subsets, but here we use a 19% subset, so access to even larger scale data could further improve results. This shows promise that in the future, our methods can leverage exponentially growing data scale to replace full ImageNet pre-training for a new pre-training method.

6. Conclusion

In this work, we proposed filtering methods to efficiently pre-train on large scale datasets conditioned on the transfer learning task. To further improve pre-training efficiency, we proposed decreased image resolution for pre-training and found this shortens pre-training cost by 30-50% with similar transfer learning accuracy. Additionally, we introduced sequential pre-training to improve the efficiency of conditional pre-training with multiple target tasks. Finally, we demonstrated how our methods can improve the standard ImageNet pre-training by focusing models pre-trained on ImageNet on relevant examples and filtering an ImageNet-sized dataset from a larger scale dataset.

References

- [1] William H Beluch, Tim Genewein, Andreas Nürnberger, and Jan M Köhler. The power of ensembles for active learning in image classification. In *Proceedings of the IEEE Conference on Computer Vision and Pattern Recognition*, pages 9368–9377, 2018. 2
- [2] Mathilde Caron, Ishan Misra, Julien Mairal, Priya Goyal, Piotr Bojanowski, and Armand Joulin. Unsupervised learning of visual features by contrasting cluster assignments. *Advances in Neural Information Processing Systems*, 33, 2020. 1
- [3] Ting Chen, Simon Kornblith, Mohammad Norouzi, and Geoffrey Hinton. A simple framework for contrastive learning of visual representations. *arXiv preprint arXiv:2002.05709*, 2020. 1, 2
- [4] Xinlei Chen, Haoqi Fan, Ross Girshick, and Kaiming He. Improved baselines with momentum contrastive learning. *arXiv preprint arXiv:2003.04297*, 2020. 1, 2
- [5] Xinlei Chen, Haoqi Fan, Ross Girshick, and Kaiming He. Improved baselines with momentum contrastive learning. *arXiv preprint arXiv:2003.04297*, 2020. 2
- [6] Gordon Christie, Neil Fendley, James Wilson, and Ryan Mukherjee. Functional map of the world. In *Proceedings of the IEEE Conference on Computer Vision and Pattern Recognition*, pages 6172–6180, 2018. 5
- [7] Yin Cui, Yang Song, Chen Sun, Andrew Howard, and Serge Belongie. Large scale fine-grained categorization and domain-specific transfer learning. In *Proceedings of the IEEE conference on computer vision and pattern recognition*, pages 4109–4118, 2018. 1, 2, 3, 4, 5, 8
- [8] Jia Deng, Wei Dong, Richard Socher, Li-Jia Li, Kai Li, and Li Fei-Fei. Imagenet: A large-scale hierarchical image database. In *2009 IEEE conference on computer vision and pattern recognition*, pages 248–255. Ieee, 2009. 1, 2, 5
- [9] Mark Everingham, Luc Van Gool, Christopher KI Williams, John Winn, and Andrew Zisserman. The pascal visual object classes (voc) challenge. *International journal of computer vision*, 88(2):303–338, 2010. 5
- [10] Yarin Gal, Riashat Islam, and Zoubin Ghahramani. Deep bayesian active learning with image data. *arXiv preprint arXiv:1703.02910*, 2017. 2
- [11] Weifeng Ge and Yizhou Yu. Borrowing treasures from the wealthy: Deep transfer learning through selective joint fine-tuning. In *Proceedings of the IEEE conference on computer vision and pattern recognition*, pages 1086–1095, 2017. 1, 2, 3, 4
- [12] Jean-Bastien Grill, Florian Strub, Florent Altché, Corentin Tallec, Pierre Richemond, Elena Buchatskaya, Carl Doersch, Bernardo Avila Pires, Zhaohan Guo, Mohammad Gheshlaghi Azar, et al. Bootstrap your own latent—a new approach to self-supervised learning. *Advances in Neural Information Processing Systems*, 33, 2020. 1
- [13] Aditya Grover, Jiaming Song, Ashish Kapoor, Kenneth Tran, Alekh Agarwal, Eric J Horvitz, and Stefano Ermon. Bias correction of learned generative models using likelihood-free importance weighting. In *Advances in Neural Information Processing Systems*, pages 11058–11070, 2019. 4
- [14] Kaiming He, Haoqi Fan, Yuxin Wu, Saining Xie, and Ross Girshick. Momentum contrast for unsupervised visual representation learning. *arXiv preprint arXiv:1911.05722*, 2019. 1, 2, 5
- [15] Kaiming He, Haoqi Fan, Yuxin Wu, Saining Xie, and Ross Girshick. Momentum contrast for unsupervised visual representation learning. In *Proceedings of the IEEE/CVF Conference on Computer Vision and Pattern Recognition*, pages 9729–9738, 2020. 1, 2, 5, 6, 7, 8
- [16] Dan Hendrycks, Kimin Lee, and Mantas Mazeika. Using pre-training can improve model robustness and uncertainty. *arXiv preprint arXiv:1901.09960*, 2019. 1, 2
- [17] Geoffrey Hinton, Oriol Vinyals, and Jeff Dean. Distilling the knowledge in a neural network. *arXiv preprint arXiv:1503.02531*, 2015. 2

- [18] Minyoung Huh, Pulkit Agrawal, and Alexei A Efros. What makes imagenet good for transfer learning? *arXiv preprint arXiv:1608.08614*, 2016. 1, 2
- [19] Simon Kornblith, Jonathon Shlens, and Quoc V Le. Do better imagenet models transfer better? In *Proceedings of the IEEE conference on computer vision and pattern recognition*, pages 2661–2671, 2019. 1, 2
- [20] Jonathan Krause, Michael Stark, Jia Deng, and Li Fei-Fei. 3d object representations for fine-grained categorization. In *Proceedings of the IEEE international conference on computer vision workshops*, pages 554–561, 2013. 5
- [21] Alina Kuznetsova, Hassan Rom, Neil Alldrin, Jasper Uijlings, Ivan Krasin, Jordi Pont-Tuset, Shahab Kamali, Stefan Popov, Matteo Mallocci, Alexander Kolesnikov, and et al. The open images dataset v4. *International Journal of Computer Vision*, 128(7):1956–1981, Mar 2020. 8
- [22] Tsung-Yi Lin, Michael Maire, Serge Belongie, James Hays, Pietro Perona, Deva Ramanan, Piotr Dollár, and C Lawrence Zitnick. Microsoft coco: Common objects in context. In *European conference on computer vision*, pages 740–755. Springer, 2014. 8
- [23] Dhruv Mahajan, Ross Girshick, Vignesh Ramanathan, Kaifeng He, Manohar Paluri, Yixuan Li, Ashwin Bharambe, and Laurens van der Maaten. Exploring the limits of weakly supervised pretraining. In *Proceedings of the European Conference on Computer Vision (ECCV)*, pages 181–196, 2018. 1, 2
- [24] Jiquan Ngiam, Daiyi Peng, Vijay Vasudevan, Simon Kornblith, Quoc V Le, and Ruoming Pang. Domain adaptive transfer learning with specialist models. *arXiv preprint arXiv:1811.07056*, 2018. 1, 2, 3
- [25] Mijung Park and Jonathan Pillow. Bayesian active learning with localized priors for fast receptive field characterization. *Advances in neural information processing systems*, 25:2348–2356, 2012. 2
- [26] Vishnu Sarukkai, Anirudh Jain, Burak Uz Kent, and Stefano Ermon. Cloud removal from satellite images using spatiotemporal generator networks. In *The IEEE Winter Conference on Applications of Computer Vision*, pages 1796–1805, 2020. 5
- [27] Ozan Sener and Silvio Savarese. Active learning for convolutional neural networks: A core-set approach. *arXiv preprint arXiv:1708.00489*, 2017. 2
- [28] Evan Sheehan, Burak Uz Kent, Chenlin Meng, Zhongyi Tang, Marshall Burke, David Lobell, and Stefano Ermon. Learning to interpret satellite images using wikipedia. *arXiv preprint arXiv:1809.10236*, 2018. 1
- [29] Hoo-Chang Shin, Holger R Roth, Mingchen Gao, Le Lu, Ziyue Xu, Isabella Nogueira, Jianhua Yao, Daniel Mollura, and Ronald M Summers. Deep convolutional neural networks for computer-aided detection: Cnn architectures, dataset characteristics and transfer learning. *IEEE transactions on medical imaging*, 35(5):1285–1298, 2016. 1, 2
- [30] Hugo Touvron, Andrea Vedaldi, Matthijs Douze, and Hervé Jégou. Fixing the train-test resolution discrepancy. In *Advances in Neural Information Processing Systems*, pages 8252–8262, 2019. 5
- [31] Burak Uz Kent and Stefano Ermon. Learning when and where to zoom with deep reinforcement learning. In *Proceedings of the IEEE/CVF Conference on Computer Vision and Pattern Recognition*, pages 12345–12354, 2020. 5
- [32] Burak Uz Kent, Aneesh Rangnekar, and Matthew J Hoffman. Tracking in aerial hyperspectral videos using deep kernelized correlation filters. *IEEE Transactions on Geoscience and Remote Sensing*, 57(1):449–461, 2018. 2
- [33] Burak Uz Kent, Evan Sheehan, Chenlin Meng, Zhongyi Tang, Marshall Burke, David Lobell, and Stefano Ermon. Learning to interpret satellite images in global scale using wikipedia. *arXiv preprint arXiv:1905.02506*, 2019. 2
- [34] Burak Uz Kent, Evan Sheehan, Chenlin Meng, Zhongyi Tang, Marshall Burke, David B Lobell, and Stefano Ermon. Learning to interpret satellite images using wikipedia. In *IJCAI*, pages 3620–3626, 2019. 2
- [35] Burak Uz Kent, Christopher Yeh, and Stefano Ermon. Efficient object detection in large images using deep reinforcement learning. In *The IEEE Winter Conference on Applications of Computer Vision*, pages 1824–1833, 2020. 5
- [36] Grant Van Horn, Oisín Mac Aodha, Yang Song, Yin Cui, Chen Sun, Alex Shepard, Hartwig Adam, Pietro Perona, and Serge Belongie. The inaturalist species classification and detection dataset. In *Proceedings of the IEEE conference on computer vision and pattern recognition*, pages 8769–8778, 2018. 5
- [37] Keze Wang, Dongyu Zhang, Ya Li, Ruimao Zhang, and Liang Lin. Cost-effective active learning for deep image classification. *IEEE Transactions on Circuits and Systems for Video Technology*, 27(12):2591–2600, 2016. 2
- [38] P. Welinder, S. Branson, T. Mita, C. Wah, F. Schroff, S. Belongie, and P. Perona. Caltech-UCSD Birds 200. Technical Report CNS-TR-2010-001, California Institute of Technology, 2010. 5
- [39] Michael Xie, Neal Jean, Marshall Burke, David Lobell, and Stefano Ermon. Transfer learning from deep features for remote sensing and poverty mapping. *arXiv preprint arXiv:1510.00098*, 2015. 1, 2
- [40] Xi Yan, David Acuna, and Sanja Fidler. Neural data server: A large-scale search engine for transfer learning data. In *Proceedings of the IEEE/CVF Conference on Computer Vision and Pattern Recognition (CVPR)*, June 2020. 1, 2, 8
- [41] Bolei Zhou, Agata Lapedriza, Aditya Khosla, Aude Oliva, and Antonio Torralba. Places: A 10 million image database for scene recognition. *IEEE transactions on pattern analysis and machine intelligence*, 40(6):1452–1464, 2017. 8